A R C H I V E S O F M E T A L L U R G Y A N D M A T E R I A L S
Volume 55 2010 Issue 1

D. PIECZABA*, A. JACH**

EVALUATION OF SUPERALLOY INCONEL 713C DENDRITIC MICROSTRUCTURE OF THE TURBINE BLADE CASTINGS

OCENA MIKROSTRUKTURY DENDRYTYCZNEJ ODLEWÓW ŁOPATEK TURBIN Z NADSTOPU INCONEL 713C

The influence of the crystallization conditions on microstructure of Inconel 713 C superalloy was presented in the paper. Turbine blades with airfoil section width of 22 and 30 mm and length of 50 mm were casted in investment molds in a vacuum furnace. The secondary dendrite arm spacing was determined through microscopic examinations. On the basis of obtained results it was established that prolonged process of crystallization results in an increase of microstructure constituents dispersion.

Keywords: turbine blade, superalloys, secondary dendrite arm spacing

W pracy przedstawiono wyniki badań wpływu warunków krystalizacji na mikrostrukturę odlewniczego stopu Inconel 713 C. Łopatki turbin o szerokości pióra 22 i 30 mm i długości pióra 50 mm wykonano metodą wytapianych modeli w piecu próżniowym. Dyspersję składników mikrostruktury określono poprzez pomiar odległości ramion dendrytów wtórnych.

1. Introduction

Inconel 713 C belongs to the group of vacuum melted Ni-based superalloys. It was developed in the 1950s, and due to its extraordinary properties it was widely used in different high temperature applications even as a blade material [1].

Dendritic microstructure of alloy Inconel 713 C consists of grains of solid solution γ – the nickel austenite with Mo, Cr, Co, Fe as well as the phase γ'(Ni, Ti, Ta, V)$_3$Al. It was reported, that the relative volume of phase γ' after heat-treatment amounts up to 65%. Moreover, the carbides of type M_6C, M_7C_3, $M_{23}C_6$ are present in microstructure formed by Mo, W and Cr, as well as carbides of type MC, which are formed by Ti and Zr. The inclusions in superalloy Inconel 713 C castings are Al or Cr oxides, formed in the reaction of alloy with material of crucible or mould. Eutectic $\gamma - \gamma$' accours in interdendritic spaces [2-4].

Dendrites arms spacing influence on the mechanical properties. Macrosegregation and interdendritic porosity are connected with the interdenritic fluid flow [5]. Those problems will be investigate in future works.

The conditions of volumetric crystallization of dendrites have an influence on their dispersion. The local over-cooling of liquid alloy enlarges time of incubation of crystallization of secondary dendrites arms, and the time of crystallization influences on their average tip distance [6]. Additionally the phenomena of mutual blocking, breaking and torsion of dendrites tips take place during the process.

2. Materials and methodology of investigations

The castings of the superalloy Inconel 713 C turbine blades with the 22 and 30 mm width and the 50 mm length were obtained by the investment casting method. The chemical composition of the alloy was presented in table 1. Three model sets were assembled from pouring cup, round top gate, three venters and 12 models of blades (6 models with the 30 mm width and 6 models with the 22 mm width) (Fig. 1). Models of blades were made of A7-FR/60 and models of gating system were made of B405 wax.

* DEPARTMENT OF MATERIAL SCIENCE, THE FACULTY OF MECHANICAL ENGINEERING AND AERONAUTICS, RZESZOW UNIVERSITY OF TECHNOLOGY, 35-959 RZESZÓW, 2 W. POLA STR., POLAND
** LABORATORY OF MATERIAL INVESTIGATION FOR THE AVIATION INDUSTRY, 35-959 RZESZÓW, 2 W. POLA STR., POLAND

TABLE 1

Chemical composition of the Inconel 713 C superalloy

Content of elements, wt. %																		
Ni	Cr	Co	Mo	W	Ta	Nb	Al	Ti	Fe	Mn	Si	C	B	Zr	Cd	Cu	Pt	V
Bal.	14	0,4	4,2	0,2	0,05	–	6,2	0,8	0,02	0,001	0,01	0,17	0,012	0,1	2	0,001	0,003	0,003

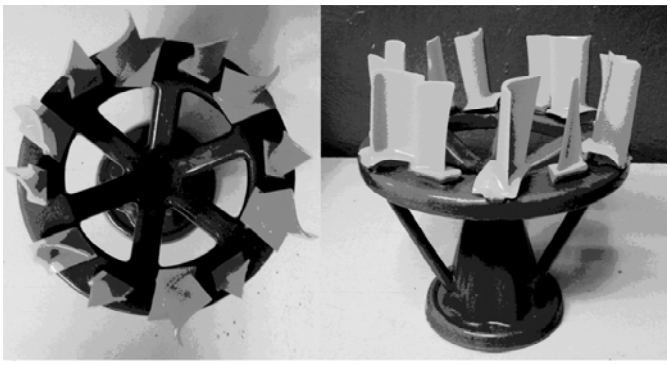

Fig. 1. Wax model set

Ceramic coats were put on by hand (9 layers). The were used the masses Alundum Elektrokorund 100 – first two layers and Molochite 30/80 and 16/30 on remaining, bonded by the colloidal silica or hydrolyzed ethyl silicate. First sand layer adjacent to the model had the content of cobalt aluminates about 10%. It is the modifier of microstructure of surface layer of the turbine blade casting. The thickness of side of ceramic mould averaged to about 6mm. Wax was smelted in autoclave and then moulds were annealed at the temperature of 1150°C by 0.5 h.

It was accepted three variants of ceramic moulds with and without insulation (Fig. 2). Insulation was made of Fiberfrax material thickness with 13 mm and density 64 kg/m^3 with addition of ZD glue.

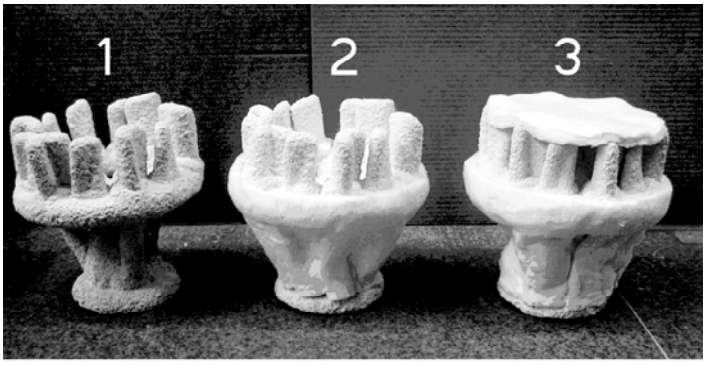

Fig. 2. Ceramic moulds subject to investigations: 1 – without thermal insulation, 2 – insulation of gating system, 3 – insulation of gating system and bottom of the mould

Insulated moulds were annealed in oven-type furnace CGE – VSM02 (Tab. 2). After annealing ceramic mould were placed in vacuum chamber of casting furnace Balzers VSG25P and were filled with melted superalloy Inconel 713 C at temperature of 1470°C and pressure about 2 Pa. Ten minutes after casting moulds were taken out from the furnace and were air-cooled for 6,5 h. The after-cast treatment (the shakeout, cut and sandblasting the castings) and the heat-treatment of castings were carried out (Tab. 3). To evaluate microstructure of turbine blades, metallographic specimens were prepared from chosen areas (Fig. 3 and 4).

TABLE 2

Conditions of annealing of the ceramic moulds in oven-type furnance CGE – VSM02
Chemical composition of the Inconel 713 C superalloy

	Loading zone	Annealing zone	Unloading zone
Temperature, ° C	400	700	400
Time, h	0.5	1.5	0.5

TABLE 3

Conditions of heat-treatment of castings made of superalloy Inconel 713 C

Stage	Pressure, Pa	Temperature, °C	Soaking time, min
1	0,12	–	10
2	0,12	650	10
3	0,12	720	10
4	78	980	10
5	78	1080	31
6	78	50	Cooling from furnace to temperature 50 ∘C
7	49996	50	3

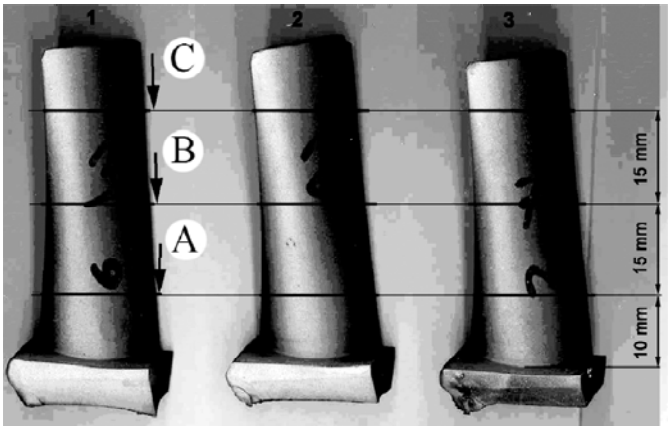

Fig. 3. The pattern of cut of turbine blade casting with dimensions of 22x50 mm

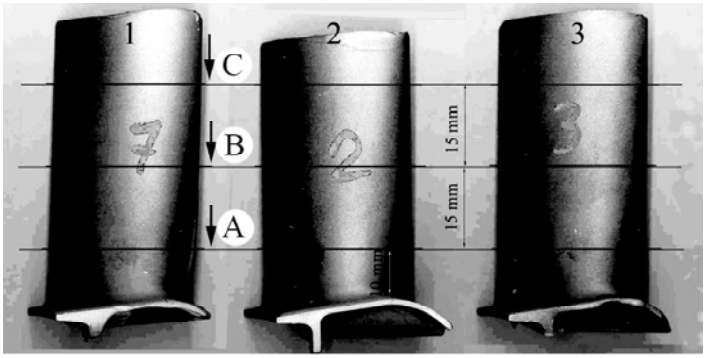

Fig. 4. The pattern of cut of turbine blade casting with dimensions of 30x50 mm

Metallographic specimens were etched by reagent "Kawasaki" (100 g of boride of iron, 0.6 dm^3 of hydrochloric acid, 0.5 dm^3 of distilled water). The examination of microstructure of turbine blades was carried out using the light microscope Nikon Epiphot 300 equipped with system of digital image recording DC -1U as well as program for numeric analysis of microscopic image NIS – Elements. The measurements of secondary dendrites arm spacing were carried out in various areas of turbine blades castings (Fig. 5 and 6). The observation was performed with magnification of 50x (Fig. 7) or 100x Fig. 8) in dependence on thickness of section of turbine blade.

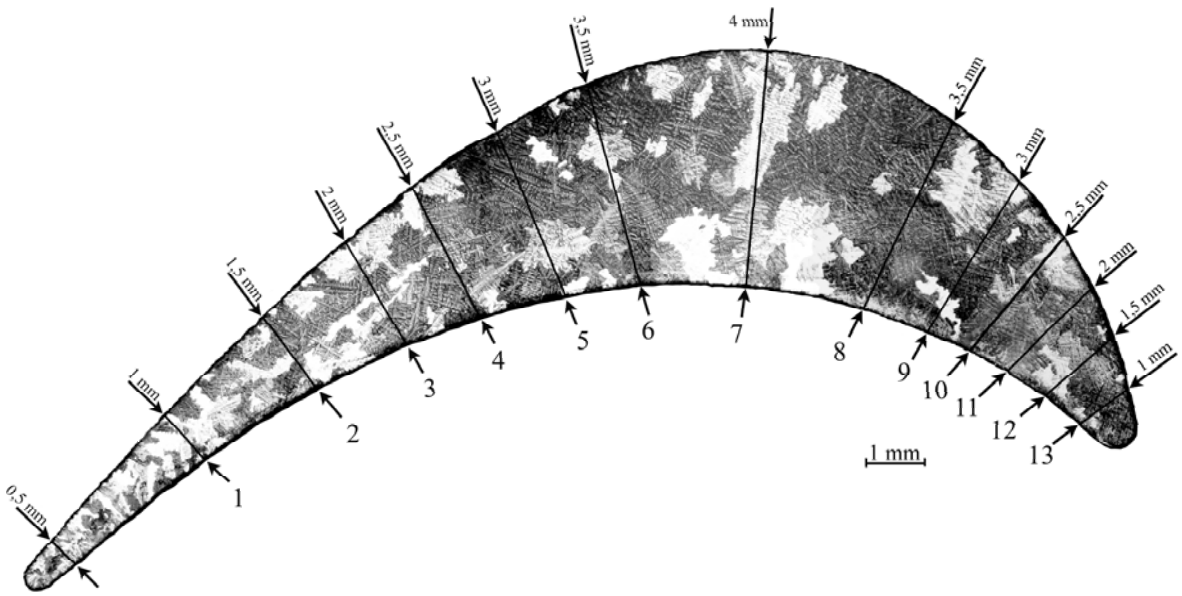

Fig. 5. The macrostructure of turbine blade casting with dimensions of 22x50 mm from superalloy Inconel 713 C (cut A – Fig. 4). 1 – 13 – the areas of dendrites arm spacing measurement

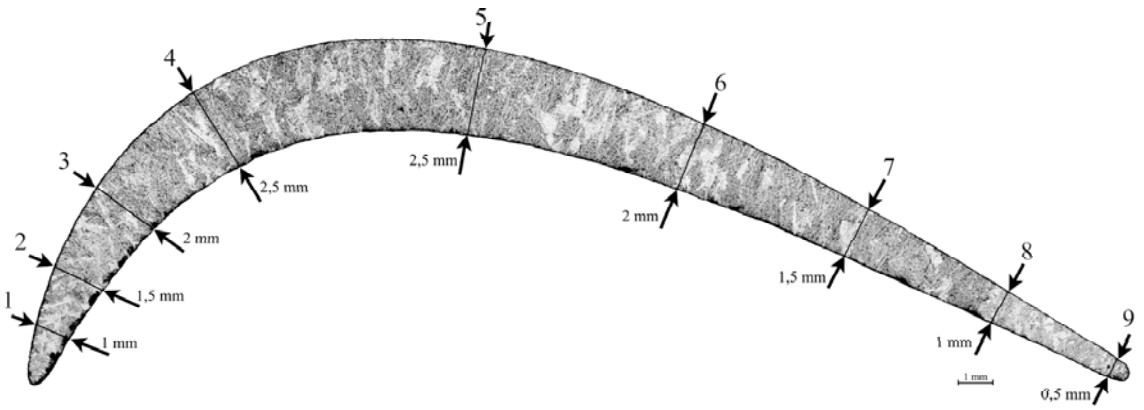

Fig. 6. The macrostructure of turbine blade casting with dimensions of 30x50 mm from superalloy Inconel 713 C (cut C – Fig. 5). 1 – 9 – the areas of dendrites arm spacing measurement

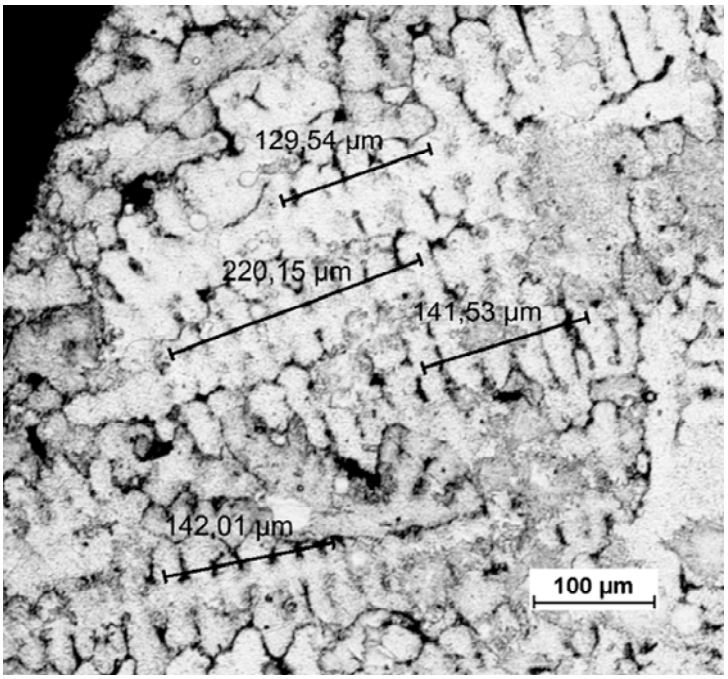

Fig. 7. The microstructure of turbine blade casting from superalloy Inconel 713 C – the measurement of secondary dendrites arm spacing

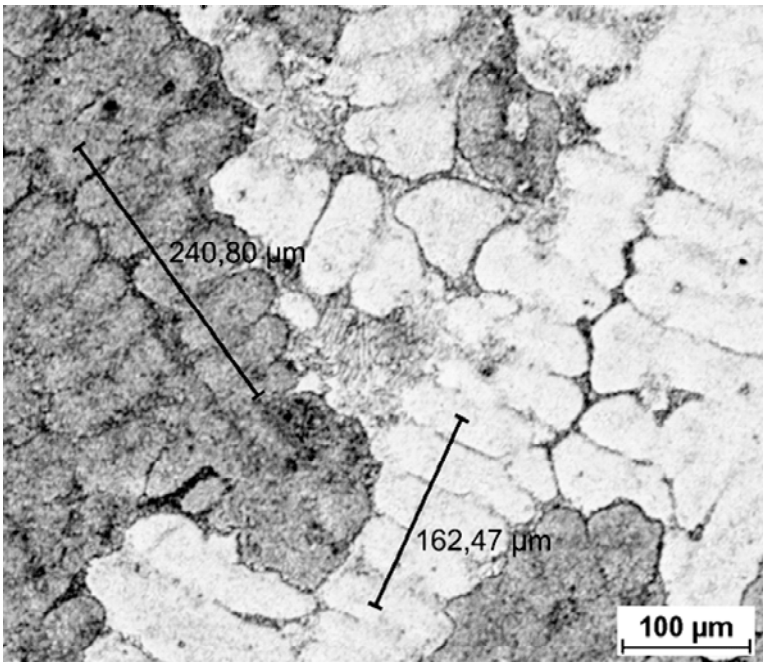

Fig. 8. The microstructure of turbine blade casting from superalloy Inconel 713 C – the measurement of secondary dendrites arm spacing

Average secondary dendrites arm sparing λ_{2i} was calculated using formula:

$$\lambda_{2i} = \frac{L}{n-1}, \tag{1}$$

where: L – secondary dendrites arm spacing, n – numbers of secondary dendrites arms.

The standard deviations s and the coefficient of changeability W were also calculated [7]:

$$s = \sqrt{\frac{1}{k-1}\Sigma(\lambda_{2i} - \bar{\lambda}_2)^2} \tag{2}$$

$$W = \frac{s}{\bar{\lambda}_2} x100\%, \tag{3}$$

where: k – the number of measurements on thickness of turbine blade, $\bar{\lambda}_2$ – the arithmetical mean distance between secondary dendrites arms on thickness of turbine blade.

It was accepted based on own investigation and literature data that the speed of growth of secondary dendrites arms on top of primary dendrite arm was quasi – linear (Fig. 9). It was due to unstable conditions of growth of primary dendrite arms. The average spacing of first twenty arms of secondary dendrites on top was constant [8,9].

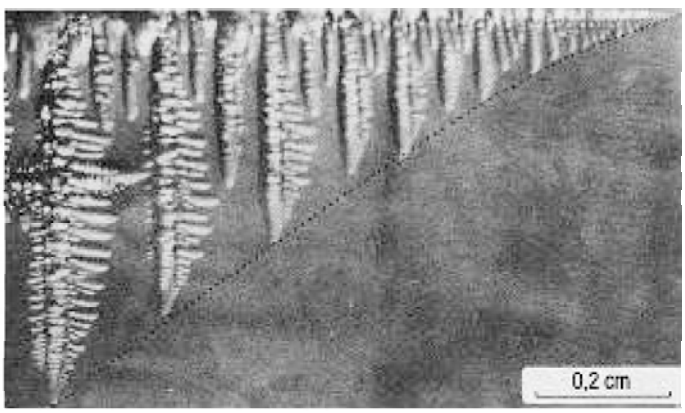

Fig. 9. Primary dendrite arm with secondary and third row dendrites arms [10]

Spacing of secondary dendrites arms is coarsened with growth of distance from top of main dendrite arm. Degree of fragmentation of dendrites arms were also enlarged. Coalescence of secondary dendrites arms was cause of this [5].

3. Results of investigations and their discussion

Measurements of secondary dendrites arms spacing in this work were carried out on primary dendrite tip and in his vicinity. This assumption was indispensable to set the correlation of interdendritic distances with conditions of crystallization. The measurement of secondary dendrites arm spacing was performed for different areas of casting (Fig. 5 and 6). The results of measurements were presented in Table 4 and 5 as well as in Fig. 10-15.

TABLE 4

The results of measurements of turbine blade castings with dimensions of 22X50 mm

Section	Ceramic mould								
	Without insulation			Insulation of gating system			Insulation of gating system and the bottom of the mould		
	Thickness of turbine blade, mm			Thickness of turbine blade, mm			Thickness of turbine blade, mm		
	The standard deviation s, μm			The standard deviation s, μm			The standard deviation s, μm		
	The coefficient of changeability W, %			The coefficient of changeability W, %			The coefficient of changeability W, %		
	1	2.7780	9	1	4.5582	12	1	3.2942	9
A	1.5	4.4026	13	1.5	4.8475	11	1.5	6.2224	15
	2	4.3310	13	2	1.3981	3	2	7.1222	16
	2.5	5.0610	14	2.5	4.2135	9	2.5	4.3492	9
	3	3.0026	8	3	4.1355	9	3	4.1845	9
	3.5	7.2570	19	3.5	5.1624	11	3.5	6.6036	14
	4	4.9945	12	4	5.0531	10	4	5.4783	11
B	1	2.0643	11	1	1.8333	10	1	2.2528	11
	1.5	3.4210	14	1.5	2.1124	9	1.5	1.6137	7
	2	2.2603	9	2	4.0835	16	2	2.7910	11
	2.5	3.2137	12	2.5	3.3418	12	2.5	2.8706	10
C	1	2.3084	14	1	1.1831	7	1	2.2556	13
	1.5	3.9603	18	1.5	3.4219	16	1.5	2.9280	13
	2	3.2368	13	2	1.4532	6	2	1.8270	8

TABLE 5

The results of measurements of turbine blade castings with dimensions of 30X50 mm

Section	Ceramic mould								
	Without insulation			Insulation of gating system			Insulation of gating system and the bottom of the mould		
	Thickness of turbine blade, mm			Thickness of turbine blade, mm			Thickness of turbine blade, mm		
	The standard deviation s, μm			The standard deviation s, μm			The standard deviation s, μm		
	The coefficient of changeability W, %			The coefficient of changeability W, %			The coefficient of changeability W, %		
A	1	–	–	1	3.4051	16	1	1.3397	6
	1.5	3.9972	16	1.5	2.9274	10	1.5	2.1941	8
	2	2.6218	9	2	2.3385	6	2	1.5856	5
	2.5	2.0092	7	2.5	1.3519	4	2.5	1.6985	5
B	1	2.1864	13	1	1.7985	10	1	2.3211	12
	1.5	1.7335	8	1.5	4.1051	17	1.5	2.1851	10
	2	2.2977	8	2	2.3243	8	2	2.3436	9
	2.5	2.2478	8	2.5	2.3694	7	2.5	3.0720	11
C	1	3.2365	19	1	2.6027	16	1	2.5104	14
	1.5	3.7156	17	1.5	4.3124	19	1.5	2.7993	13
	2	2.6316	10	2	3.6761	14	2	1.8061	7
	2.5	2.7579	10	2.5	3.0010	11	2.5	2.8414	9

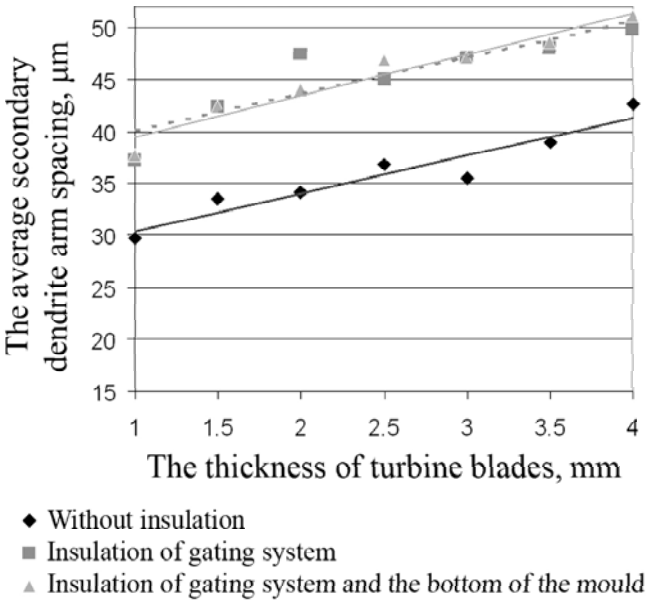

Fig. 10. The influence of thickness of turbine blades with the 22 mm width on the average secondary dendrite arm spacing. Section A (Fig. 4)

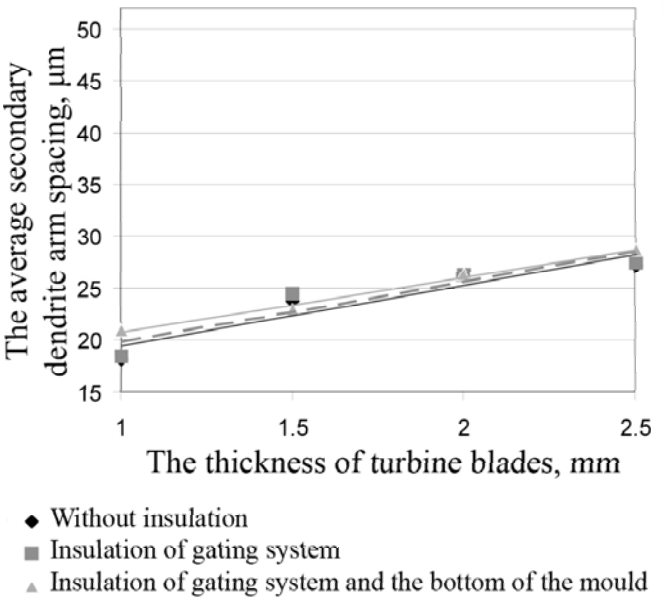

Fig. 11. The influence of thickness of turbine blades with the 22 mm width on the average secondary dendrite arm spacing. Section B (Fig. 4)

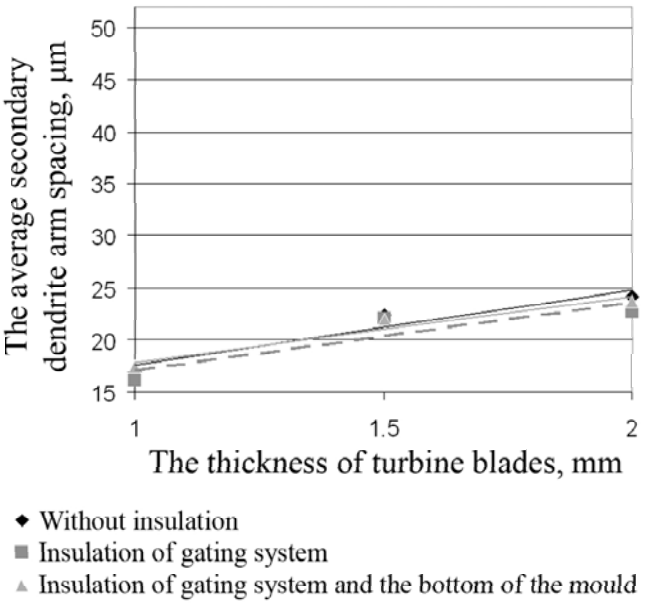

Fig. 12. The influence of thickness of turbine blades with the 22 mm width on the average secondary dendrite arm spacing. Section C (Fig. 4)

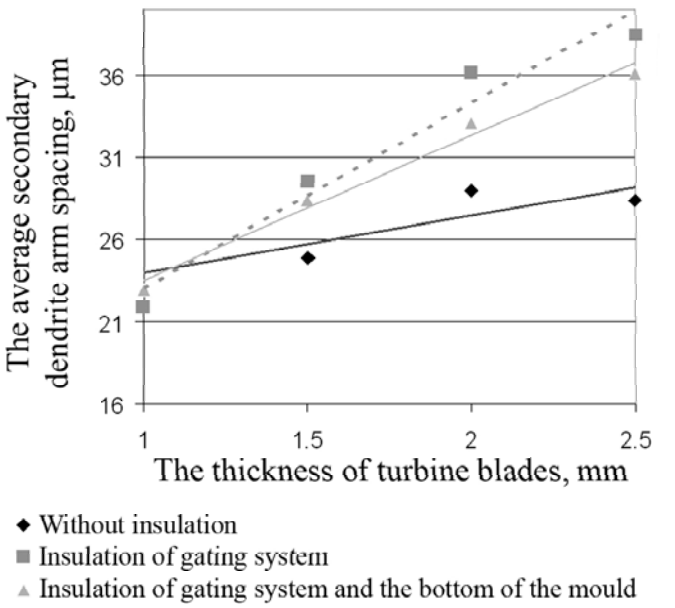

Fig. 13. The influence of thickness of turbine blades with the 30 mm width on the average secondary dendrite arm spacing. Section A (Fig. 5)

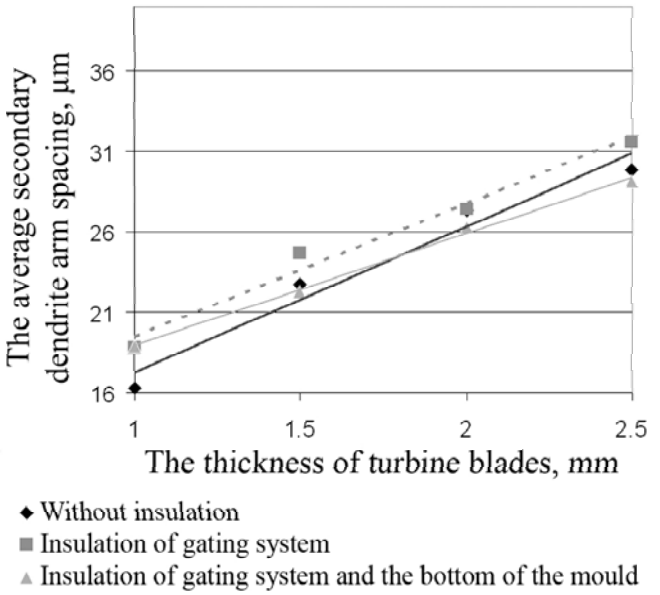

Fig. 14. The influence of thickness of turbine blades with the 30 mm width on the average secondary dendrite arm spacing. Section B (Fig. 5)

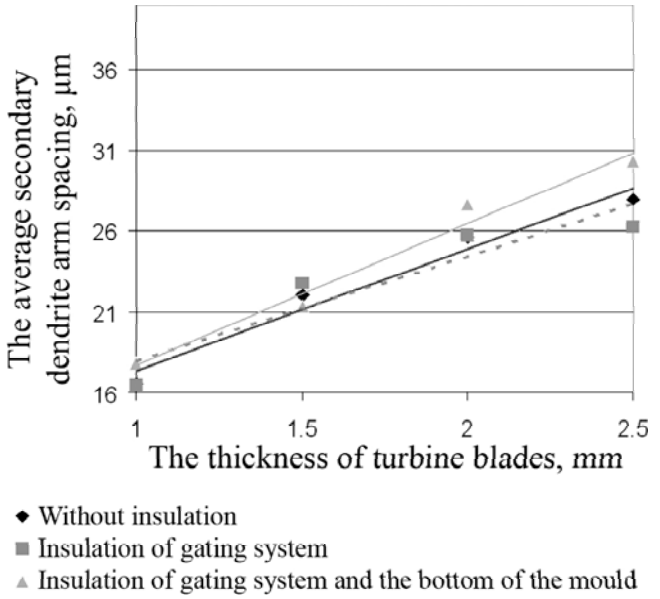

Fig. 15. The influence of thickness of turbine blades with the 30 mm width on the average secondary dendrite arm spacing. Section C (Fig. 5)

The results of investigations permitted to affirm, that the conditions of crystallization (the variable wall thickness of casting and method of the insulation of mould) of the turbine blades castings made of superalloy Inconel 713 C have the influence on their microstructure. The close relationship of heat exchange conditions with the microstructure of castings was affirmed. On sections A of turbine blades, in places of casting situated at the top of the mould, the influence of insulation of gating system of mould on secondary dendrites arm spacing was observed. The significant influence of insulates on sections of casts situated lower in mould was not affirmed. The influence of wall thickness of turbine blade on dispersion of microstructure was observed – the larger was the wall thickness of turbine blade then secondary dendrite arm coarsening was observed.

4. Conclusions

The use of Fiberfrax insulation in ceramic casting moulds has influence on kinetics of crystallization process of superalloy Inconel 713 C castings. Insulation of gating system of moulds causes decreasing the crystallization rate and enlargement of the feeding of lower parts of casting (section A). The larger time of crystallization leads to enlargement of average secondary dendrites arms spacing. The use of insulation of bottom part of the mould does not influence on crystallization kinetics in lower parts of casting (section C). The wall thickness of turbine blades has large influence on microstructure of alloy Inconel 713 C. The greater is the wall thickness of turbine blade, the greater secondary dendrites arms spacing is obtained.

REFERENCES

[1] Alloy Digest, Data on world wide metals and alloys, Inconel 713C, February, 1959.

[2] B. Mikułowski, Stopy żaroodporne i żarowytrzymałe – nadstopy, Wydawnictwa AGH, Kraków 1997.

[3] A. Hernas, Żarowytrzymałość stali i stopów cz.I. Wydawnictwo Politechniki Śląskiej, Gliwice 2000.

[4] JM. Hochmann, Aciers et alliages réfractaires. Tech Ing 1981;MB4:M325-32.

[5] ASM Handbook, vol. **15** Casting, 1988.

[6] E. Fraś, Krystalizacja metali., Wydawnictwa Naukowo-Techniczne, Warszawa, 2003.

[7] J. Ryś, Stereologia materiałów, Fotobiti-Design, Kraków 1995.

[8] C. Beckermann, Q. Li, Acta Metall. **47**, 2345 (1999).

[9] A. Wagner, B. A. Shollock, M. McLean, Grain structure development in directional solidification of nickel-base superalloys. Materials Science and Engineering **A 374**, 270-279 (2004).

[10] S. Huang, M. Glicksman, Acta Metalurgica **29**, 717 (1981).

Received: 10 September 2009.